Food & Medicine Homology

ISSN 3006-6867 (print); 3006-4252 (online)
https://doi.org/10.26599/FMH.2027.9420171

Research Article

Uncovering the anti-inflammatory mechanism of Jiang-Huang-Qing-Yan-Yin (JHQYY) in inflammatory bowel disease through network pharmacology, molecular docking, and cellular verification

Meng-Ru Liu[1, 2, †], Yi-Ning Feng[1, 2, †], Tao Sun[1, 2], Bo Wang[1, 2], Wei-Kang Yang[1, 2], Wei Xue[1, 2], Tian-Zhu Guan[1, 2] (✉), Dan Xiong[1, 2] (✉)

[1] *College of Food Science and Engineering, Yangzhou University, Yangzhou* 225127, *China*
[2] *Yangzhou Engineering Research Center of Food Intelligent Packaging and Preservation Technology, Yangzhou University, Yangzhou* 225127, *China*
[†] *Meng-Ru Liu and Yi-Ning Feng contributed equally to this work.*

Received: 5 November 2025 / **Revised:** 23 April 2026 / **Accepted:** 2 May 2026

Abstract: Inflammation is a key driver of immune responses; however, its dysregulation can lead to chronic diseases such as inflammatory bowel disease (IBD). This study investigates the anti-inflammatory and antioxidant effects of Jiang-Huang-Qing-Yan-Yin (JHQYY), a multi-component herbal formula, using network pharmacology, molecular docking and cellular verification. Network pharmacology identified the main active ingredients: Tea polyphenols, vitamin E, vitamin C and caffeine, as well as their associated targets in JHQYY, revealing 44 compounds and 850 potential targets. Among these, 64 common targets were identified between JHQYY and IBD. Protein-protein interaction (PPI) network analysis highlighted key targets, including IL-6, TNF, ALB, and IL1B, which are critical in the pathogenesis of IBD. Gene Ontology (GO) and Kyoto Encyclopedia of Genes and Genomes (KEGG) pathway analyses identified significant inflammatory and immune regulatory pathways, particularly the NF-κB and IL-17 signaling pathways. Molecular docking further confirmed that key active components, such as tea polyphenols and caffeine, exhibit strong interactions with inflammatory targets like TNF and ALB. JHQYY displayed strong antioxidant activity, with the aqueous extract showing superior ABTS radical scavenging capacity, while the alcohol extract demonstrated higher ferric-reducing antioxidant power (FRAP). Additionally, the cellular experiments demonstrated that JHQYY exhibited low cytotoxicity in RAW264.7 macrophages, significantly inhibited lactate dehydrogenase (LDH) release, and reduced the expression levels of pro-inflammatory cytokines (IL-1β, IL-6, TNF-α) induced by lipopolysaccharide (LPS). This research emphasizes that JHQYY has the potential to act as a natural anti-inflammatory substance and provides preliminary *in vitro* evidence supporting its anti-inflammatory potential relevant to IBD.

Keywords: inflammatory bowel disease; network pharmacology; JHQYY; molecular docking; anti-inflammation; cellular verification

Citation: Liu M. R., Feng Y. N., Sun T., et al. Uncovering the anti-inflammatory mechanism of Jiang-Huang-Qing-Yan-Yin (JHQYY) in inflammatory bowel disease through network pharmacology, molecular docking, and cellular verification. *Food & Medicine Homology*, 2027, 4: 9420171. https://doi.org/10.26599/FMH.2027.9420171

1 Introduction

Inflammation is a defense mechanism against infection, injury, or foreign insults[1,2], primarily mediated by immune system activation[3]. Key immune cells (e.g., macrophages, neutrophils, T cells) drive this process by secreting pro-inflammatory cytokines (TNF-α, IL-1β, IL-6), which clear pathogens and initiate tissue repair[4]. However, dysregulated inflammation may cause tissue damage, contributing to diseases like inflammatory bowel disease (IBD), rheumatoid arthritis, and sepsis[5]. As pivotal innate immune cells, macrophages detect pathogens *via* pattern recognition receptors (PRRs)[6]. For instance, TLR4 binding by lipopolysaccharide (LPS) activates NF-κB signaling, amplifying cytokine production[7]. Thus, modulating this axis could mitigate inflammatory damage.

Traditional nonsteroidal anti-inflammatory drugs (NSAIDs) and corticosteroids, while demonstrating significant anti-inflammatory effects, are often associated with severe side effects such as gastrointestinal damage, immune suppression, and metabolic disorders when used long-term[8,9]. Traditional Chinese medicine (TCM) herbal formulations are increasingly recognized for their anti-inflammatory potential, attributed to multi-component synergism[10]. Curcumin, the primary bioactive compound in *Curcuma longa*, suppresses pro-inflammatory cytokine release *via* dual inhibition of NF-κB nuclear translocation and MAPK phosphorylation[11-13]. Epigallocatechin gallate (EGCG), found in green tea, effectively reduces the production of inflammatory mediators by inhibiting NF-κB activation[14]. Glycyrrhizin, a compound in licorice, exerts anti-inflammatory

Address correspondence to Tian-Zhu Guan, guantz@yzu.edu.cn; Dan Xiong, xiongdan@yzu.edu.cn

effects by modulating the expression of cytokines such as TNF-α, IL-6, and IL-1β[15]. Other studies have shown that *Poria cocos* can reduce the production of inflammatory factors and alleviate inflammation-induced damage by inhibiting the NF-κB signaling pathway, as well as repair the intestinal barrier[16]. Cinnamaldehyde, found in cinnamon, reduces IL-1β release by inhibiting NLRP3 inflammasome activation[17,18]. However, single-herb interventions often face significant clinical limitations, such as poor oral bioavailability or narrow target specificity, which limits their efficacy in complex systemic diseases like IBD. In contrast, the Jiang-Huang-Qing-Yan-Yin (JHQYY) formula integrates these distinct mechanisms—combining the metabolic regulation of flavonoids with the immune-suppressive power of polyphenols—to create a "multi-target, multi-pathway" therapeutic network. These natural active ingredients, through their combined action, may offer a complementary approach for modulating inflammation. However, the specific contribution and interaction of individual components within this formulation remain to be experimentally elucidated.

The complexity of natural bioactive compounds makes it challenging to fully elucidate their anti-inflammatory mechanisms through traditional pharmacological methods. Network pharmacology integrates systems biology, bioinformatics, and multi-omics approaches to map "drug-target-disease" interactions, thereby deciphering the polypharmacology of natural compounds. Studies have revealed that *Pueraria lobata* suppresses inflammation *via* HSP90AA1-mediated MAPK/mTOR/NF-κB inhibition, as confirmed by network analysis and wet-lab validation[19]. Similarly, allocryptopine demonstrates anti-inflammatory effects in a dextran sulfate sodium-induced mouse model by targeting the CX3CL1-CX3CR1 axis/GNB5/AKT/NF-κB/apoptosis pathway[20]. Moreover, network pharmacology can be employed to optimize the formulation of TCM compounds, analyzing the synergistic effects of different ingredients to screen the best combinations for enhancing anti-inflammatory effects. The integration of network pharmacology and molecular docking can identify potential drug targets. For example, bipyridyl ketone, through network pharmacology and molecular docking analysis, may regulate multiple signaling pathways to treat IBD[21]. Similarly, the lipophilic fraction of *Liriope platyphylla* seeds has demonstrated antioxidant and anti-inflammatory potential by modulating targets such as NFKB1, PTGS1, and PTGS2[22]. The combination of network pharmacology and molecular docking also shows great potential in TCM anti-inflammatory research. For instance, the Juanbi formula has been shown to alleviate the inflammatory response in rheumatoid arthritis by inhibiting the AP-1 and NF-κB signaling pathways[23]. Therefore, the integration of network pharmacology and molecular docking techniques holds significant application value in anti-inflammatory research.

This study employed network pharmacology and molecular docking to construct a component-target-disease network for herbal compounds containing *Curcuma longa* L. (Jianghuang), *Camellia sinensis* (L.) Kuntze (Lücha), *Glycyrrhiza uralensis* Fisch. ex DC. (Gancao), *Wolfiporia cocos* (Fuling), *and Cinnamomum cassia* (L.) J.Presl (Rougui). This approach aimed to identify key anti-inflammatory targets and pathways, elucidating the anti-inflammatory mechanism of the active compounds. Additionally, cytotoxicity effects of the JHQYY compound on RAW264.7 macrophages were assessed, along with lactate dehydrogenase (LDH) release levels. The anti-inflammatory effect of the compound was evaluated by measuring the release of inflammatory cytokines in LPS-induced RAW264.7 cells. This study provides a new research direction for the development of natural anti-inflammatory compounds to alleviate inflammatory responses.

2 Materials and methods

2.1 Identification of active chemical composition and molecular targets of JHQYY

The JHQYY, including Jianghuang, Lücha, Rougui, Fuling and Gancao (used as search keywords here), was imported into the Traditional Chinese Medicine Systems Pharmacology Database and Analysis Platform (TCMSP) (https://tcmspw.com/tcmsp.php)[24] and HERB (http://herb.ac.cn/). To identify compounds with high oral bioavailability and drug similarity, compounds with an oral bioavailability (OB) ≥ 30% and drug-likeness (DL) ≥ 0.18 were selected[25]. Given the considerable number of Gancao compounds that met these criteria and the limited number for Rougui, the screening parameters for these two herbs were modified. Targets corresponding to these compounds were obtained from the TCMSP and HERB databases.

2.2 Prediction of targets for IBD

Using IBD as the search term, relevant targets were retrieved from the human gene databases, GeneCards, (https://www.genecards.org/)[26] and MalaCards (https://www.malacards.org/)[27]. Following this, the common targets with JHQYY and IBD were determined using Venny 2.1.0.

2.3 Construction of PPI network

A protein–protein interaction (PPI) network of potential accommodative targets was generated and initially analyzed using STRING 12.0 (https://cn.string-db.org/)[28]. Species were limited to "*Homo sapiens*" with a minimum interaction score exceeding 0.4 (highest confidence level). Upon the establishment of the PPI network, the results were imported into Cytoscape for further visualization.

2.4 Enrichment analysis

To explore the key signaling pathways and biological processes of JHQYY in the regulation of IBD, Gene Ontology (GO) and Kyoto Encyclopedia of Genes and Genomes (KEGG) pathway enrichment analyses were performed using STRING 12.0 (https://cn.string-db.org/)[28]. GO functional annotation analysis was conducted to categorize the genes into biological processes, molecular functions, and cellular components (CCs). KEGG pathway enrichment analysis was subsequently performed to identify the primary pathways associated with these genes. The integration of GO and KEGG enrichment analyses offers functional insights into a large number of genes from a broader perspective, facilitating the identification of drug-disease signaling pathways and potential therapeutic targets for IBD.

2.5 Molecular docking

Molecular docking was adopted *via* AutoDock Vina[29] to further clarify the link between active components and key genes and to access the intensity and mode of interaction. The top few JHQYY compounds with the most potential to regulate IBD and predicted targets were selected for molecular docking. The proteins were discarded off water and added with polar hydrogens and demanded charges *via* AutoDock Tools. Then the minimum

binding energy was searched *via* Autodock Vina. Generally, a negative value of binding energy represents a stable level of ligand binding to the receptor. The binding effect is better when the score is higher.

2.6 Molecular dynamics (MD) simulation

To validate the dynamic stability of the caffeine-ALB complex predicted by molecular docking, a 100 ns all-atom MD simulation was performed using GROMACS 2023.3. The ALB crystal structure (PDB: 1AO6, Chain A) was prepared by removing water molecules and heteroatoms. Protein topology was generated with the AMBER99SB-ILDN force field, and caffeine parameters were assigned using GAFF2/ACPYPE with AM1-BCC partial charges. The system was solvated in a TIP3P water box (1.0 nm padding) and neutralized with 0.15 mol/L NaCl. Energy minimization (steepest descent) was followed by NVT (100 ps, 300 K, V-rescale) and NPT (100 ps, 1 bar, Parrinello-Rahman) equilibration with positional restraints on heavy atoms. The 100 ns production run used a 2 fs time step, PME electrostatics, and a 1.0 nm van der Waals cutoff. Backbone RMSD, per-residue RMSF, number of intermolecular contacts, and minimum ligand-protein distance were calculated using built-in GROMACS tools. The final 50 ns were used for equilibrium analysis.

2.7 *In silico* metabolic profiling

To assess the metabolic fate of key JHQYY bioactive compounds, *in silico* metabolic profiling was performed using BioTransformer 3.0 (https://biotransformer.ca), which predicts human Phase I and Phase II metabolic reactions based on experimentally validated enzyme knowledge bases. Three representative compounds, including caffeine, cinnamaldehyde, and curcumin were submitted as SMILES strings, and the predicted metabolites, metabolic enzymes, and reaction types were exported for analysis.

2.8 Extraction of JHQYY bioactives

Based on the TCM principle of "Jun-Chen-Zuo-Shi" (Monarch-Minister-Assistant-Guide) to optimize synergistic efficacy, the JHQYY, including Jianghuang, Lücha, Rougui, Fuling and Gancao was mixed in a weight ratio of 3:2:2:2:1. The formulation was ground into a fine powder and soaked in either 70% ethanol or distilled water at ambient temperature for 12 h. Ultrasonic-assisted extraction (UAE) was conducted based on the protocol reported by Liu *et al*.[30]. To ensure the preservation of thermolabile bioactive components identified *in silico* and the reproducibility of the chemical profile, a standardized UAE protocol was employed[31]. Extraction was performed at 40 °C for 80 min using an ultrasonic cleaner working at a frequency of 40 kHz and power of 300 W with a solid-to-liquid ratio of 1:15. These specific parameters were selected based on optimized yields for heat-sensitive polyphenols and polysaccharides reported in the literature, ensuring efficient mass transfer while preventing the thermal degradation of active constituents. The resulting solution was filtered and subsequently subjected to vacuum freeze-drying at −50 °C for 72 h to obtain the final powder.

2.9 Determination of antioxidant capacity

2.9.1 *ABTS assay*

In the ABTS assays, the samples were evaluated at five concentration levels: 0.01, 0.1, 1, 2.5, 5, and 10 mg/mL. For data analysis, all concentrations were logarithmically transformed and applied to plot dose-response curves to assess antioxidant activity trends. The $ABTS^+$ (2,2'-azino-bis(3-ethylbenzothiazoline-6-sulfonic acid) radical scavenging activity was assessed following the protocol established by Binsan *et al*.[32] A stock solution comprising 7 mmol/L ABTS and 2.45 mmol/L potassium persulfate ($K_2S_2O_8$) was prepared by combining equal amounts of both reagents. The mixture was kept in the dark at ambient temperature for 12–16 h to generate $ABTS^+$ radicals. The solution was then diluted with anhydrous ethanol until its absorbance reached 1.4 ± 0.02 at 405 nm. For the assay, 10 μL of the sample was mixed with 200 μL of the diluted $ABTS^+$ working solution. The reaction mixture was incubated in the dark at room temperature for 2–6 min. The $ABTS^+$ scavenging rate (%) was determined using the following formula:

$$\text{ABTS radical scavenging rate}\,(\%) = \left(1 - \frac{A_1 - A_2}{A_0}\right) \times 100\%$$

In the formula, A_1 represents the absorbance of 10 μL of the extraction sample mixed with 200 μL of ABTS working solution, followed by a 20-min reaction at room temperature in the dark. A_0 is the absorbance of 10 μL of distilled water mixed with 200 μL of ABTS solution. A_2 is the absorbance of 200 μL of distilled water mixed with 10 μL of the sample.

2.9.2 *DPPH assay*

In the 1,1-diphenyl-2-picrylhydrazyl (DPPH) assays, the samples were tested at five concentration gradients: 0.1, 1, 2.5, 5, 10, and 20 mg/mL. The IC_{50} (half-maximal inhibitory concentration) values were calculated using nonlinear regression analysis. The DPPH radical scavenging activity was determined as described in Alzagameem *et al*[33]. A 0.2 mmol/L DPPH solution was prepared in anhydrous ethanol. For the assay, 2.9 mL of the DPPH solution was mixed with 0.1 mL of the test sample in a 10 mL test tube. The mixture was vortexed thoroughly and incubated at room temperature for 30 min. The absorbance (A_1) was measured at 517 nm using a spectrophotometer. A control experiment was conducted by replacing the sample solution with 0.1 mL distilled water to obtain the absorbance (A_0). Additionally, the absorbance of 0.1 mL of the sample solution mixed with 2.9 mL anhydrous ethanol was measured at 517 nm as A_2. The DPPH radical scavenging rate (%) was calculated using the following formula:

$$\text{DPPH radical scavenging rate}\,(\%) = \left(1 - \frac{A_1 - A_2}{A_0}\right) \times 100\%$$

2.9.3 *FRAP assay*

To determine the antioxidant index using the ferric-reducing antioxidant power (FRAP) assay, the samples were tested at concentrations of 1, 2, 5, 8, and 10 mg/mL. The assay was conducted following the method described by Yang *et al*[34]. First, the following solutions were prepared: Trolox standard, 300 mmol/L acetate buffer (24.6 g of sodium acetate dissolved in 700 mL ultrapure water, pH adjusted to 3.6 with acetic acid), 10 mmol/L TPTZ, and 20 mmol/L ferric chloride. The working solution was made by mixing these solutions in a 10:1:1 ratio just before use. For total antioxidant capacity determination, $FeSO_4$ was used as the standard, and a calibration curve was generated using $FeSO_4$ solutions in distilled water at six concentrations (0.15, 0.3, 0.6, 0.9, 1.2, and 1.5 mmol/L). The assay was performed in 96-well microplates, with each well receiving 180 μL of freshly prepared FRAP working solution. Then, 5 μL aliquots were added

according to the experimental design: (a) blank controls received distilled water, (b) standard curve wells contained $FeSO_4$ solutions, and (c) sample wells contained test samples or 0.15–1.5 mmol/L Trolox as the positive control. The mixture was incubated at 37 °C for 3–5 min, and the absorbance was measured at 593 nm. Total antioxidant capacity was calculated using the standard curve. Samples outside the standard curve range were diluted before measurement. The actual absorbance was obtained by subtracting the blank value from the measured absorbance.

2.10 Cell culture

RAW264.7 macrophages were purchased from American Type Culture Collection (ATCC, Cat# TIB-71). The cells were cultured in DMEM medium (Gibco, California, USA) supplemented with 10% fetal bovine serum (FBS) and maintained in a humidified incubator at 37 °C with 5% CO_2. When cell confluence reached 80%–90%, subculturing was performed.

2.11 Cytotoxicity assay

To evaluate the cytotoxicity of the compound formula on RAW264.7 cells, the 3-(4,5-dimethylthiazol-2-yl)-2,5-diphenyltetrazolium bromide (MTT) assay was performed. RAW264.7 cells were seeded into 96-well plates at a density of 5×10^4 cells/well and incubated overnight. The cells were then treated with the anti-inflammatory compound at concentrations of 1, 2, 4, and 8 mg/mL for 3 h. After treatment, the supernatant was removed, and 10 μL of MTT solution along with 90 μL of fresh medium was added to each well, followed by a 4-h incubation. Subsequently, the supernatant was discarded, and 110 μL of formazan solvent was added to each well. The plates were gently shaken at low speed for 10 min to fully dissolve the formazan crystals. Absorbance was measured at 490 nm using a microplate reader. All samples were tested in triplicate.

The concentration range used in the *in vitro* assays was selected as a preliminary screening scope to evaluate the cytocompatibility and anti-inflammatory activity of the JHQYY extract in RAW264.7 macrophages. Based on the MTT results, 1 and 2 mg/mL, which showed no apparent cytotoxicity, were chosen as the working concentrations for subsequent functional assays.

2.12 LDH release assay

LDH release was measured using an LDH Cytotoxicity Assay Kit (Beyotime, China). RAW264.7 cells were seeded into 24-well plates at a density of 2×10^5 cells/well and incubated overnight at 37 °C in a humidified atmosphere with 5% CO_2. The freeze-dried JHQYY powder was dissolved in sterile distilled water to prepare a stock solution and filtered through a 0.22 μm membrane. This stock solution was subsequently diluted with serum-free DMEM to obtain the final working concentrations. The cells were then treated with the anti-inflammatory compound at concentrations of 1 and 2 mg/mL for 3 h. Following treatment, 10 μL of LPS was added to each well to achieve a final concentration of 100 ng/mL, and the cells were incubated for an additional 3 h. The culture supernatant was then transferred to a new 96-well plate, and 60 μL of LDH detection working solution was added to each well. After mixing, the plate was gently shaken at low speed for 30 min at room temperature in the dark. The absorbance was measured at 495 nm, with 600 nm as the reference wavelength.

2.13 RNA extraction and qRT-PCR analysis

RAW264.7 macrophages (2×10^5 cells/well) were seeded in a 96-well plate and cultured overnight. The cells were treated with different concentrations (1, 2 mg/mL) of the anti-inflammatory compound for 3 h. Afterward, the cells were stimulated with LPS (100 ng/mL) for an additional 3 h. Total RNA was extracted using the FastPure® Cell/Tissue Total RNA Isolation Kit (Vazyme, Nanjing, China) according to the manufacturer's instructions. cDNA was synthesized using HiScript® III RT SuperMix for qPCR reagents. Quantitative real-time PCR (qRT-PCR) was performed using the AceQ Universal SYBR qPCR Master Mix (Vazyme) on a Q1000 Real-Time PCR System (LongGene, Hangzhou, China) to detect the mRNA expression levels of the cytokines *TNF-α*, *IL-1β*, *IL-6*, *p65*, *CAT*, and *SOD1*. The 20 μL reaction mixture consisted of 10 μL 2 × SYBR Premix Ex Taq II, 0.4 μL of both forward and reverse primers, 6.7 μL ddH_2O, and 2.5 μL of diluted cDNA. The PCR program was as follows: Initial denaturation at 95 °C for 5 min, followed by 40 cycles of 95 °C for 10 s and 60 °C for 30 s. The primers for qRT-PCR were synthesized by GenScript (Nanjing, China), and the primer sequences are listed in Table 1. Relative mRNA levels were normalized to the internal reference gene *GAPDH* and calculated using the $2^{-\Delta\Delta Ct}$ method.

2.14 Statistical analysis

The experimental data in this study are presented as mean ± standard deviation (mean ± SD). Statistical analysis was performed using GraphPad Prism 9.0 software. Statistical significance was determined based on the following criteria: $^*P < 0.05$, $^{**}P < 0.01$, $^{***}P < 0.001$, and the corresponding annotations are provided in the relevant figures.

3 Results and discussion

3.1 Construction of the compound-target network of JHQYY in relation to IBD

A total of 44 compounds and 850 potential related targets in JHQYY were identified using the TCMSP and HERB database. The compounds included 3 types in Jianghuang, 10 types in Lücha, 10 types in Rougui, 6 types in Fuling, and 15 types in Gancao. Then totally 292 genes associated with IBD were obtained by integrating data from MalaCards and GeneCards. Among them, 195 targets were identified the genecards whose relevance is greater than 50. From malacards, 145 targets with score greater than or equal to 100 were selected. After constructing herb disease intersection using Venny 2.1.0, 64 intersection targets of JHQYY and IBD were obtained (Fig. 1A). The active compound-target network diagram (Fig. 1B) was drawn after inputting the active compounds and common targets into Cytoscape 3.9.1. The network consists of 113 nodes and 186 edges, with Lücha having the largest number of edges (97), followed by Gancao and Rougui, which indicates that they play an integral role in the whole compound. Preliminary analysis of the network indicates a close relationship between the active ingredients in the compounds and their targets, and these three TCM raw materials potentially play the most significant role in the polyherbal formulation.

3.2 Effective compounds in JHQYY for IBD

Using the degree values from Cytoscape analysis of JHQYY, the top four components linked to the disease targets were determined (Table 2), which were tea polyphenols, vitamin C, vitamin E and caffeine.

Table 1 Primer sequences used for the quantitative real-time PCR

Primers	Sequence (5'-3')	Product size (bp)	Accession no.
GAPDH-F	AACTTTGGCATTGTGGAAGG	223	NM_001289726.2
GAPDH-R	ACACATTGGGGGTAGGAACA		
IL-1β-F	GCCCATCCTCTGTGACTCAT	230	NM_008361.4
IL-1β-R	AGGCCACAGGTATTTTGTCG		
TNF-α-F	AGCCCCCAGTCTGTATCCTT	212	NM_013693.3
TNF-α-R	CTCCCTTTGCAGAACTCAGG		
IL-6-F	AGTTGCCTTCTTGGGACTGA	159	NM_031168.2
IL-6-R	TCCACGATTTCCCAGAGAAC		
IL-10-F	CCAAGCCTTATCGGAAATGA	162	NM_010548.2
IL-10-R	TTTTCACAGGGGAGAAATCG		
p65-F	CACCGGATTGAAGAGAAGCG	194	NM_009045.5
p65-R	AAGTTGATGGTGCTGAGGGA		
CAT-F	TGGGACCCAACTATCTGCAG	248	NM_009804.2
CAT-R	TGTGTAGAATGTCCGCACCT		
SOD1-F	AACCATCCACTTCGAGCAGA	203	NM_011434.2
SOD1-R	GGTCTCCAACATGCCTCTCT		

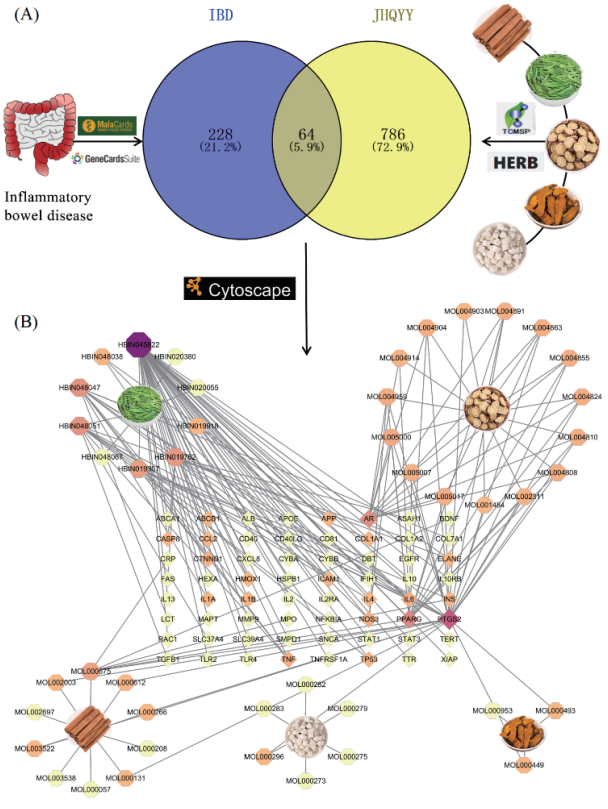

Figure 1 The common targets between JHQYY and IBD, and their network of active ingredients. (A) Possible targets of JHQYY and IBD were obtained from the database, and 64 intersection targets were obtained from Venny (B) Network of active ingredients of JHQYY and 64 intersection targets.

Studies have shown that polyphenols from green tea have potent antioxidant properties, it can also regulate the expression of TLR4 through certain receptors, inhibit the activation of NF-κB signaling pathway, and the expression of cytokines and the synthesis of COX-2, thereby inhibiting LPS-mediated TNF-α production[35]. Wu *et al.* showed in animal experiments both tea polysaccharides and tea polyphenols are promising in the treatment of IBD. Tea polysaccharides together with tea polyphenols had greater effects on alleviating colitis and promoting intestinal barrier function[36]. While these single-component studies demonstrate efficacy, they often require high doses to achieve therapeutic levels. JHQYY features a multi-component antioxidant system that combines diverse radical-scavenging mechanisms. Unlike single supplementation with vitamin C or E, JHQYY combines the hydrophilic radical scavenging of vitamin C[37] with the lipophilic protection of vitamin E[38] and Tea Polyphenols. Potential mechanisms by which vitamin E plays a role in the prevention and treatment of IBD include improving oxidative damage, enhancing immunity, maintaining intestinal barrier integrity, inhibiting inflammatory cytokines, regulating gut microbiota, and other relevant factors. This systematic integration suggests that JHQYY functions as a coordinated therapeutic formulation rather than a simple mixture, offering a broader spectrum of oxidative protection and inflammatory inhibition than previously reported single-herb formulations.

3.3 PPI network analysis of main targets in JHQYY related with IBD

To identify the potential mechanisms of JHQYY against IBD, PPI was used to analyze the correlations of JHQYY with the targets of inflammation. Totally 64 potential regulatory targets were identified (Fig. 1). The 64 shared targets between the JHQYY and IBD were input into STRING 12.0 to construct a PPI network. The resulting PPI data were imported into Cytoscape 3.9.1 to generate a comprehensive target interaction network diagram (Fig. 2). After MCODE analysis, these intersecting genes form a complete cluster. The closeness of their relationship is represented by color, and a redder color reflects a higher correlation.

TNF inhibitors have been increasingly used in IBD management[39], as TNF-α plays a central role in the inflammatory process by promoting the production of cytokines such as IL-1β and IL-6[40]. The JHQYY formula is characterized by a multi-component composition that engages multiple targets within the inflammatory network, as demonstrated by our network pharmacology analysis. Unlike single-target biological agents that

Table 2 Compounds in the ingredient-target netwok of JHQYY (top 4)

Active compound	MOL ID	Molecular formula	2D structure	Degree
Tea polyphenols	HBIN045822	$C_{22}H_{18}O_{11}$	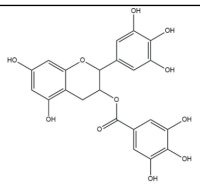	49
Vitamin E	HBIN048051	$C_{29}H_{50}O_2$	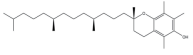	11
Vitamin C	HBIN048047	$C_6H_8O_6$	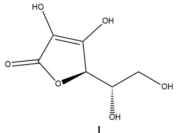	11
Caffeine	HBIN019307	$C_8H_{10}N_4O_2$	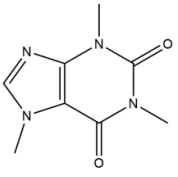	10

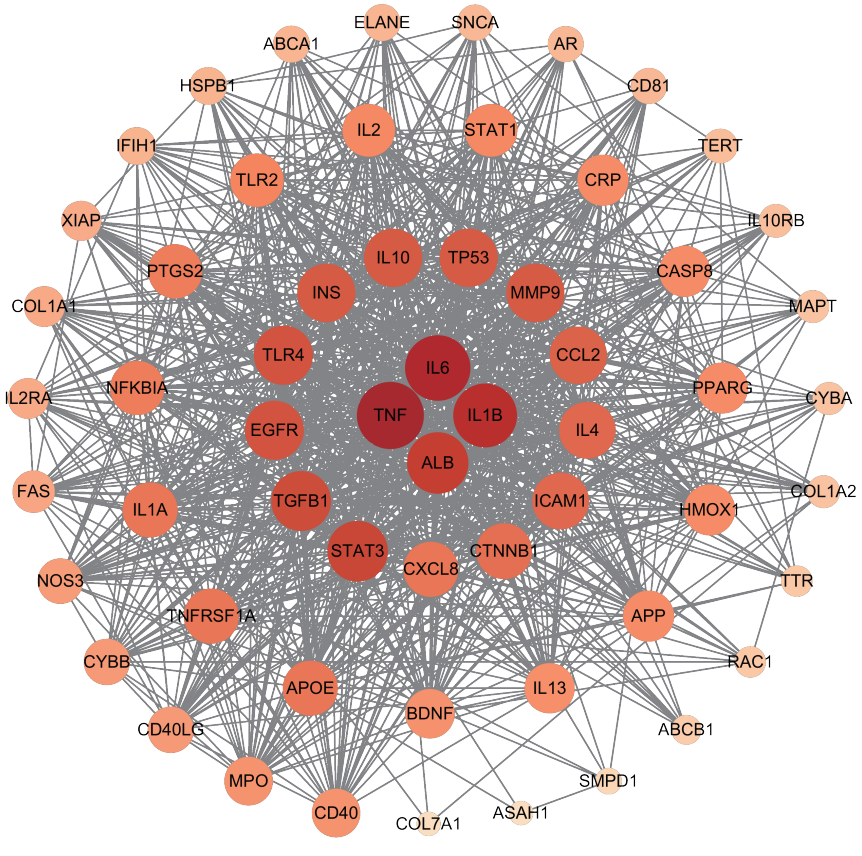

Figure 2 PPI network of intersection targets of JHQYY and IBD. A larger area represents bigger nodes, while a red hue signifies stronger association, whereas a lighter shade indicates weaker association. The core targets are located within the inner circle.

block a specific receptor, the formulation contains compounds predicted to interact with distinct nodes in the PPI network. It should be noted that while these interactions suggest the potential for coordinated multi-target regulation, the actual synergistic or additive nature of these interactions requires future experimental validation using single-component control groups. Regarding ALB, although it is a major plasma carrier protein synthesized predominantly by hepatocytes[41], the present study did not include dedicated binding assays or pharmacokinetic experiments to validate the functional significance of the docking-predicted caffeine–ALB interaction. Moreover, our additional qRT-PCR assessment showed that ALB expression in RAW264.7 macrophages was extremely low, with Ct values generally above 37, indicating that this cell model is not suitable for mechanistic evaluation of ALB-related effects. Therefore, ALB is discussed only as a network-associated factor and a docking-predicted potential binding-related molecule, rather than as a functionally validated mechanistic mediator.

3.4 GO and KEGG pathway enrichment analyses

GO enrichment analysis was performed using the STRING database, followed by the analysis of target proteins. A total of 1,329 significant GO terms were identified, comprising 1,224 biological processes (BPs), 56 CCs, and 49 molecular functions (MFs). Additionally, 121 enriched KEGG signaling pathways were identified, and the top 10 GO and KEGG terms for each category were ranked by count value (Fig. 3).

GO biological process (BP) analysis indicated that the regulatory effects of JHQYY may be mediated through inflammatory response, response to mechanical stimulus, positive regulation of cytokine production, and regulation of inflammatory response, among other processes that influence the inflammatory microenvironment of IBD (Fig. 3A). These biological processes are closely associated with the pathological mechanisms of IBD, suggesting that JHQYY may contribute to intestinal immune homeostasis by modulating excessive inflammation or enhancing anti-inflammatory responses, thereby alleviating IBD symptoms. GO molecular function (MF) enrichment analysis revealed that the target proteins of JHQYY were significantly enriched in cytokine receptor binding, cytokine activity, signaling receptor activator activity, receptor-ligand activity, signaling receptor binding, and tumor necrosis factor receptor superfamily binding (Fig. 3B). The enrichment of these molecular functions suggests that JHQYY may influence immune cell signaling and the release of inflammatory mediators by regulating cytokine receptor interactions, thereby modulating the inflammatory cascade in IBD. GO cellular component (CC) analysis indicated that the

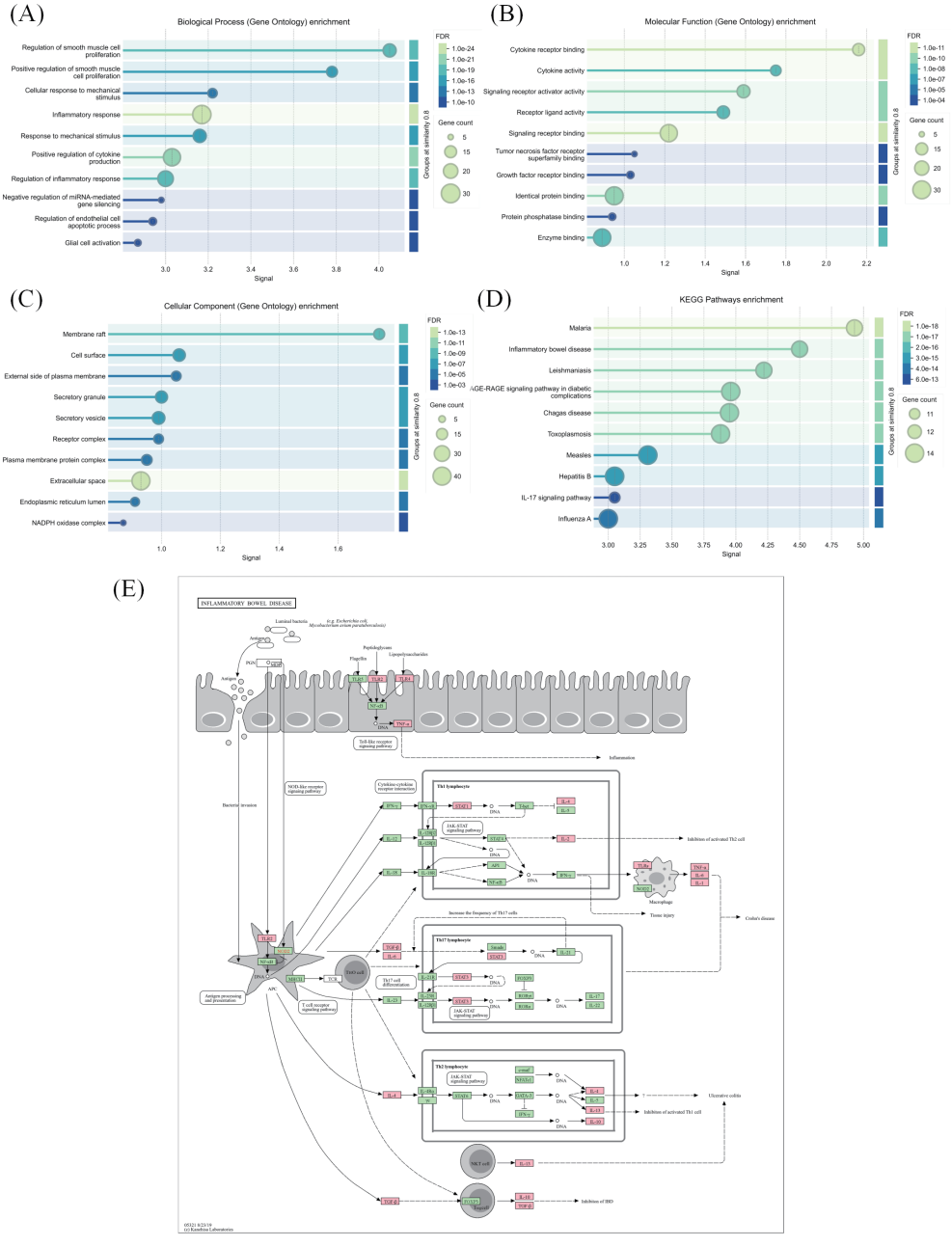

Figure 3 The GO and KEGG analyses reveal that JHQYY targets pathways involved in inflammation, immune response, and inflammatory bowel disease. (A) GO BP enrichment analysis. (B) GO MF enrichment analysis. (C) GO CC enrichment analysis. (D) KEGG pathway enrichment analysis. (E) Diagrams of the IBD signaling pathway. Emphasizing the target shared by both JHQYY and IBD, depicted in pink.

targets of JHQYY were primarily localized in the membrane raft, cell surface, external side of the plasma membrane, and secretory granules, among other CCs (Fig. 3C). GO functional analysis suggests that these target proteins, which mediate the regulatory effects of the JHQYY formula on IBD, are associated with multiple biological processes and molecular functions.

Enrichment analysis of the KEGG signaling pathway indicated that JHQYY targets the IBD pathway, IL-17 signaling pathway, AGE-RAGE signaling pathway (associated with diabetic complications), and multiple infection-related signaling pathways, including malaria, leishmaniasis, Chagas disease, toxoplasmosis, measles, hepatitis B, and influenza A (Fig. 3D). The enrichment of the IBD pathway suggests that JHQYY may be involved in IBD-related inflammatory and immune regulatory mechanisms, particularly in the modulation of pro-inflammatory factors such as TNF-α, IL-1β, and IL-6. Given the critical role of IL-17 in the immunopathological processes of IBD, the enrichment of this pathway further implies that JHQYY may influence immune dysregulation in IBD by modulating the inflammatory response mediated by Th17 cells[42].

The TCM formula JHQYY may regulate IBD through multiple pathways, primarily by modulating key inflammatory targets. Based on KEGG pathway analysis[43], the identified targets associated with this formula are predominantly involved in immune signaling cascades, including the NF-κB pathway, Th1/Th17 cell differentiation, regulatory T cell (Treg) function, and intestinal epithelial integrity (Fig. 3E). While the NF-κB signaling pathway is a shared mechanism among many anti-inflammatory agents, a notable feature of JHQYY is the predicted dual-targeting interaction identified in our network and docking analysis. The network and docking analysis suggests that JHQYY may simultaneously engage targets related to the cytokine-mediated inflammatory response (TNF *via* tea polyphenols) and systemic homeostasis markers (ALB *via* caffeine). Whether this predicted multi-target engagement translates into a genuine therapeutic advantage over single-component treatments warrants further investigation with appropriate experimental controls. The NF-κB signaling pathway plays a pivotal role in IBD pathogenesis by promoting the transcription of pro-inflammatory cytokines such as TNF-α, IL-6, and IL-1β[44]. Therefore, the therapeutic advantage of JHQYY is not merely in suppressing a common pathway, but in the coordinated contribution of specific high-affinity components to a broader regulatory network.

As a key inflammatory mediator in IBD, TNF-α contributes to epithelial barrier dysfunction and immune cell infiltration[40]. Targeting TNF-α is a well-established therapeutic approach for IBD, and bioactive compounds in JHQYY may mitigate inflammation by reducing TNF-α levels.

3.5 IBD core targets of JHQYY using molecular docking models

In order to investigate the regulatory mechanism of JHQYY against IBD and investigate the potential binding pattern and degree of binding to key targets, we conducted molecular docking of key compounds in JHQYY and core targets associated with IBD. It is widely recognized that lower binding energy signifies a more stable ligand-receptor interaction, implying a higher likelihood of the chemical engaging with the protein. To ensure reproducibility, docking simulations were performed in triplicate. The results demonstrated that the mean binding energies for Tea Polyphenols-TNF and Caffeine-ALB were −5.71 ± 0.13 kcal/mol and −5.25 ± 0.12 kcal/mol, respectively (Fig. 4).

Caffeine interacts with TYR-138 and ARG-186 *via* hydrogen bonding to form a stable bond (Fig. 5A). ALB is a major plasma carrier protein, and the predicted interaction between caffeine and ALB in the docking analysis should currently be regarded only as a potential binding possibility rather than evidence of altered

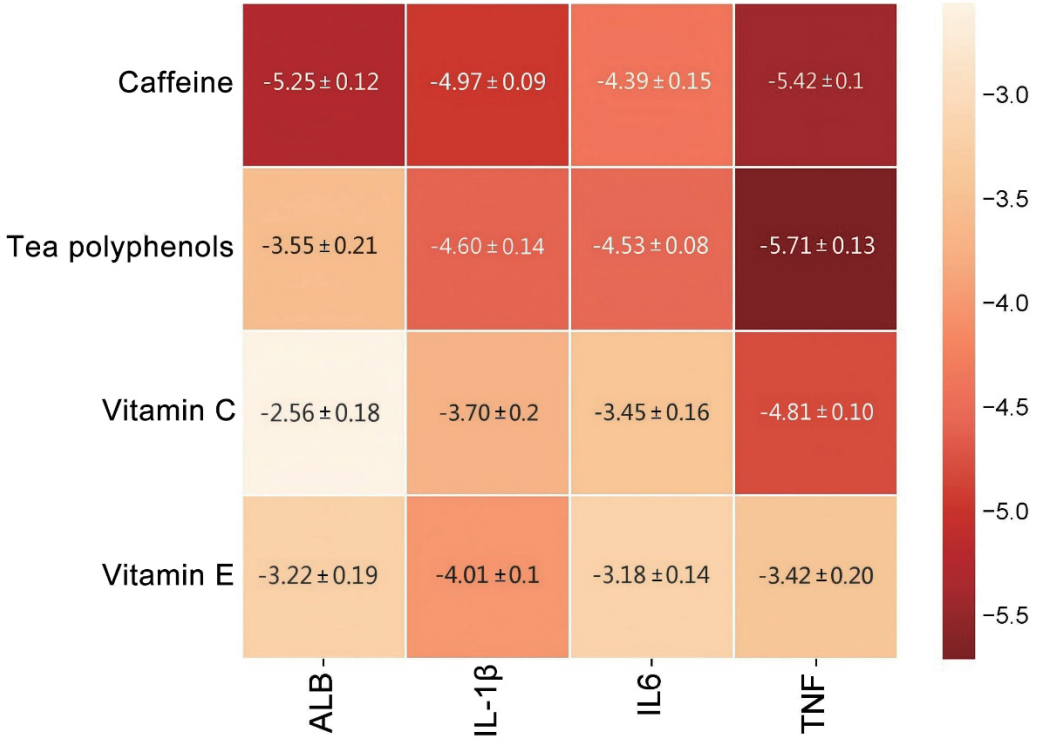

Figure 4 Molecular docking heat maps of the first four targets in the PPI network and the first four active components of JHQYY. The redder the color, the lower the binding energy and the closer the binding degree.

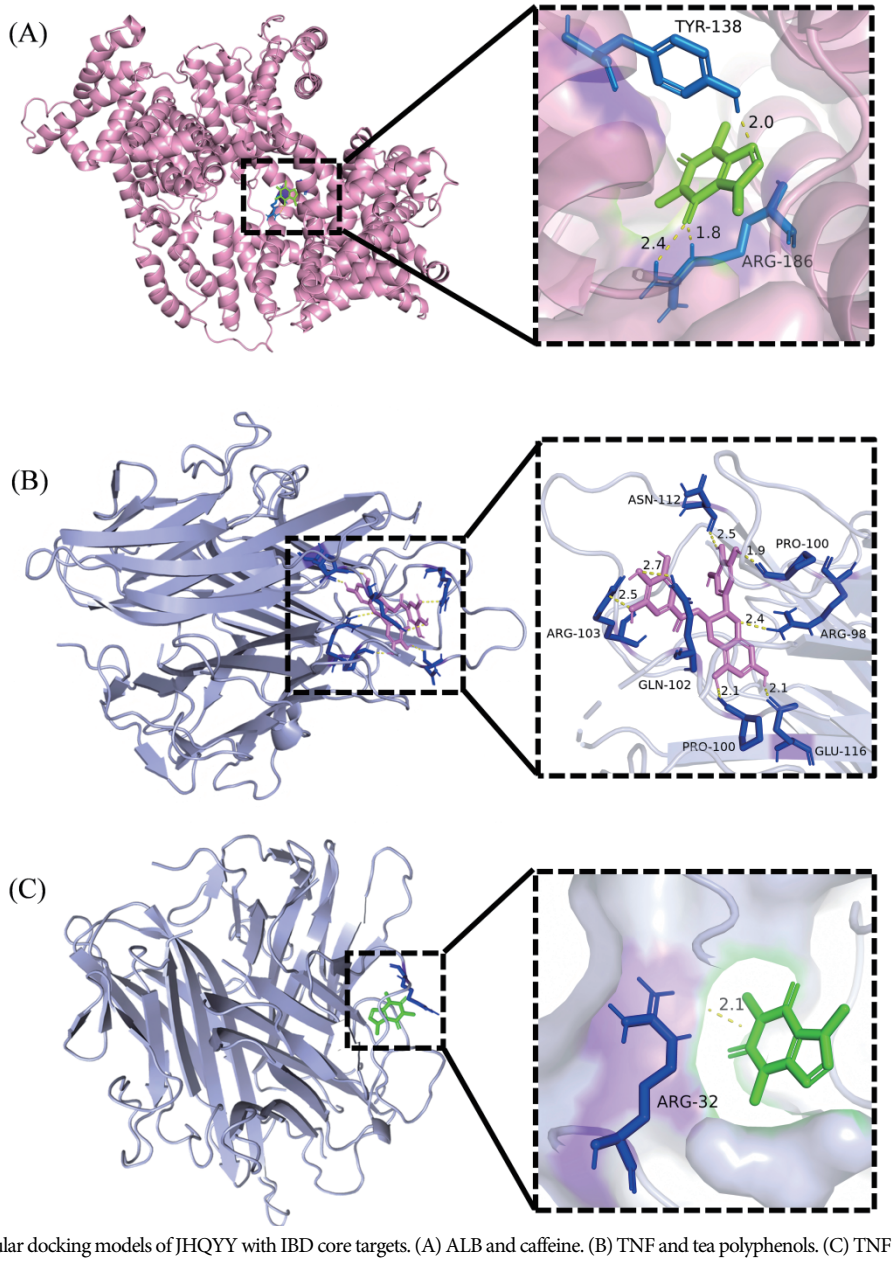

Figure 5 Molecular docking models of JHQYY with IBD core targets. (A) ALB and caffeine. (B) TNF and tea polyphenols. (C) TNF and caffeine.

stability, metabolism, or bioavailability. Tea polyphenols form multi-point interaction with ARG-98, GLN-102, ASN-112, PRO-100, GLU-116 and other amino acid residues through hydrogen bonding, and the binding pocket is deep, indicating strong affinity (Fig. 5B). Although caffeine can bind to TNF, the action site is limited, and the effect of inhibiting TNF may not be as significant as tea polyphenols (Fig. 5C). Therefore, from the perspective of molecular docking, tea polyphenols may represent an active component with greater direct anti-inflammatory potential in JHQYY, whereas the biological significance of the predicted caffeine–ALB interaction remains unclear and requires dedicated biochemical and pharmacokinetic validation.

3.6 MD simulation confirms stable caffeine-ALB binding

To evaluate whether the caffeine-ALB interaction predicted by molecular docking is maintained under physiological conditions, a 100 ns all-atom MD simulation was performed, and four metrics—backbone RMSD, per-residue RMSF, intermolecular contact number, and minimum ligand-protein distance—were monitored over the trajectory (Fig. 6).

The system reached equilibrium at approximately 25–30 ns, after which the backbone RMSD of ALB plateaued at 0.306 ± 0.025 nm for the remainder of the simulation (Fig. 6A), indicating that caffeine binding did not induce large-scale conformational changes in the protein. RMSF analysis further showed that the binding pocket residues TYR-138 and ARG-186, which form hydrogen bonds with caffeine in the docked pose, exhibited low positional fluctuation (~0.10 nm) compared to the flexible loop regions (Fig. 6B), suggesting that the local binding environment remained structurally rigid throughout the simulation. Consistent with this, the number of intermolecular contacts between caffeine and ALB was maintained at a stable average of approximately 140 with no prolonged dissociation events (Fig. 6C), and the minimum ligand-protein distance remained at ~2.4 Å (Fig. 6D), well within the range of direct van der Waals contact and

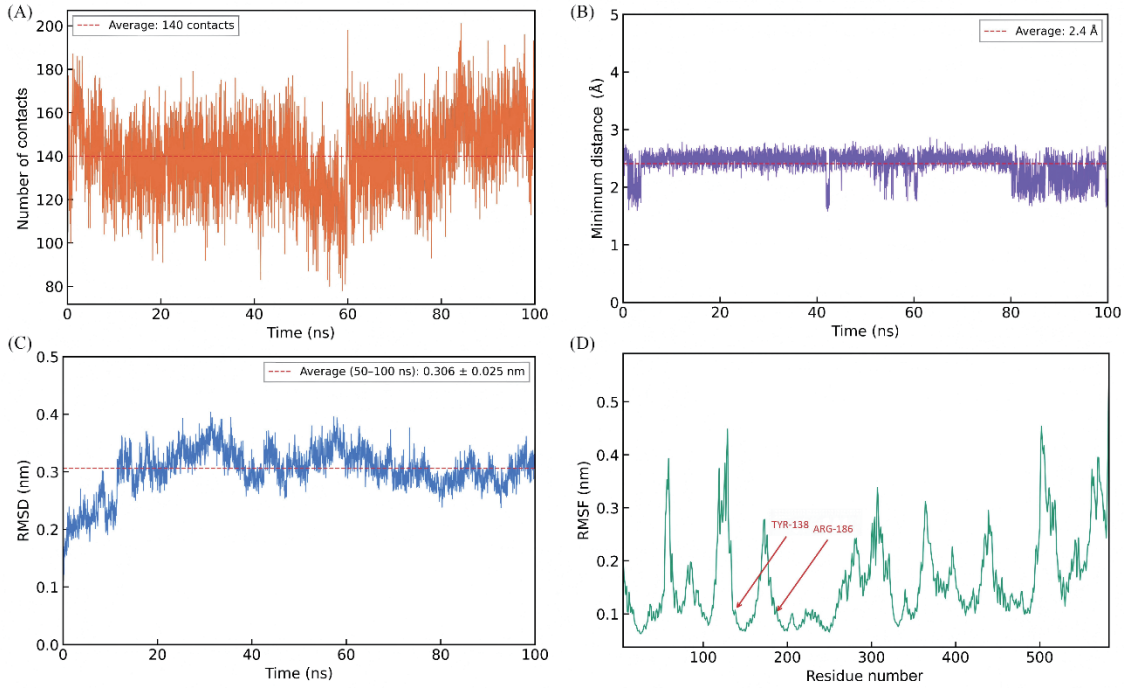

Figure 6 Molecular dynamics simulation of the caffeine-ALB complex over 100 ns. (A) Backbone RMSD; the red dashed line indicates the equilibrium average (0.306 ± 0.025 nm, 50–100 ns). (B) Per-residue RMSF; red arrows mark binding pocket residues TYR-138 and ARG-186 (RMSF ≈ 0.10 nm). (C) Number of intermolecular contacts (average: 140). (D) Minimum caffeine-ALB distance (average: 2.4 Å), confirming continuous binding throughout the simulation.

hydrogen bonding.

Taken together, these results indicate that the docking-predicted caffeine-ALB interaction is computationally stable over the 100 ns timescale. It should be noted, however, that computational binding stability does not directly imply pharmacokinetic consequences such as altered plasma half-life or tissue distribution. Experimental validation through binding assays or *in vivo* pharmacokinetic studies would be necessary to determine the functional significance of this interaction.

3.7 *In Silico* metabolic profiling supports the pharmacokinetic plausibility of JHQYY

To address the translational gap between *in vitro* concentrations and *in vivo* relevance, BioTransformer 3.0 was employed to predict the human metabolic fate of three key JHQYY compounds (Table 3). Caffeine was predicted to undergo *N*-demethylation primarily *via* CYP1A2 and CYP2D6, generating paraxanthine, theobromine, and theophylline as major Phase I metabolites, all of which are pharmacologically active methylxanthines with documented anti-inflammatory properties. Cinnamaldehyde was predicted to be rapidly metabolized *via* aldehyde oxidation to cinnamic acid and *via* reduction to cinnamyl alcohol, followed by Phase II conjugation including GSH conjugation and glycine conjugation, consistent with its known electrophilic reactivity and rapid first-pass metabolism. Curcumin exhibited the most complex metabolic profile, with 208 predicted metabolites encompassing carbonyl reduction, *β*-diketone hydrolysis to yield ferulic acid (a bioactive phenolic acid), *O*-demethylation, and extensive Phase II glucuronidation. This is consistent with the widely reported poor oral bioavailability of curcumin and its dependence on metabolite-mediated bioactivity.

Table 3 Predicted major metabolites of key JHQYY bioactive compounds by BioTransformer 3.0

Parent compound	Metabolite	Molecular formula	MW (Da)	Metabolic enzyme (s)	Reaction type	Phase
Caffeine	Paraxanthine	$C_7H_8N_4O_2$	180.06	CYP1A2, CYP2D6	*N*-Demethylation	I
Caffeine	Theobromine	$C_7H_8N_4O_2$	180.06	CYP1A2, CYP2D6	*N*-Demethylation	I
Caffeine	Theophylline	$C_7H_8N_4O_2$	180.06	CYP1A2, CYP2D6, CYP3A4	*N*-Demethylation	I
Caffeine	1,3,7-Trimethyluric acid	$C_8H_{10}N_4O_3$	210.08	CYP1A2, CYP2D6, CYP3A4	*C*-8 Hydroxylation	I
Cinnamaldehyde	Cinnamic acid	$C_9H_8O_2$	148.05	EC 1.2.3.1	Aldehyde oxidation	I
Cinnamaldehyde	Cinnamyl alcohol	$C_9H_{10}O$	134.07	EC 1.1.1.184	Aldehyde reduction	I
Cinnamaldehyde	GSH-cinnamaldehyde conjugate	$C_{19}H_{25}N_3O_7S$	439.14	EC 2.5.1.18	GSH conjugation	II
Cinnamaldehyde	Hippuric acid*	$C_9H_9NO_3$	179.06	—	Glycine conjugation	II
Curcumin	Hexahydrocurcumin	$C_{22}H_{24}O_7$	400.15	EC 1.1.1.184	Carbonyl reduction	I
Curcumin	Ferulic acid	$C_{10}H_{10}O_4$	194.06	EC 3.7.1	*β*-Diketone hydrolysis	I
Curcumin	Curcumin glucuronide	$C_{28}H_{30}O_{13}$	574.17	EC 2.4.1.17	*O*-Glucuronidation	II
Curcumin	Demethylcurcumin	$C_{21}H_{20}O_6$	384.12	CYP1A2, CYP2C9, CYP2D6	*O*-Demethylation	I

Collectively, the involvement of major drug-metabolizing CYP450 enzymes (CYP1A2, CYP2C9, CYP2D6, CYP3A4) across all three compounds confirms that these bioactives enter well-characterized human metabolic pathways. The identification of pharmacologically active metabolites—particularly paraxanthine from caffeine and ferulic acid from curcumin—provides computational evidence supporting the biological plausibility of our *in vitro* findings.

3.8 JHQYY enhances the free radical scavenging ability and shows the FRAP difference

In this study, three methods (DPPH, ABTS, and FRAP) were used to investigate and compare the antioxidant effects of JHQYY. The present research highlights the potential of JHQYY in ameliorating IBD, with a mechanistic emphasis on its antioxidant properties as evidenced by ABTS, DPPH, and FRAP assays. IBD is associated with alterations in inflammation and oxidative stress[45]. People with IBD have higher levels of oxidative stress, and excess free radicals may damage the intestinal barrier and worsen inflammation. As shown in Fig. 7, the water extract exhibited stronger ABTS radical scavenging activity than the alcohol extract, with an IC_{50} of 0.533,9 mg/mL compared to 2.385 mg/mL for the alcohol extract. In the DPPH assay, both extracts showed weaker radical scavenging activity, with the water extract exhibiting slightly better performance (IC_{50} = 4.228 mg/mL) than the alcohol

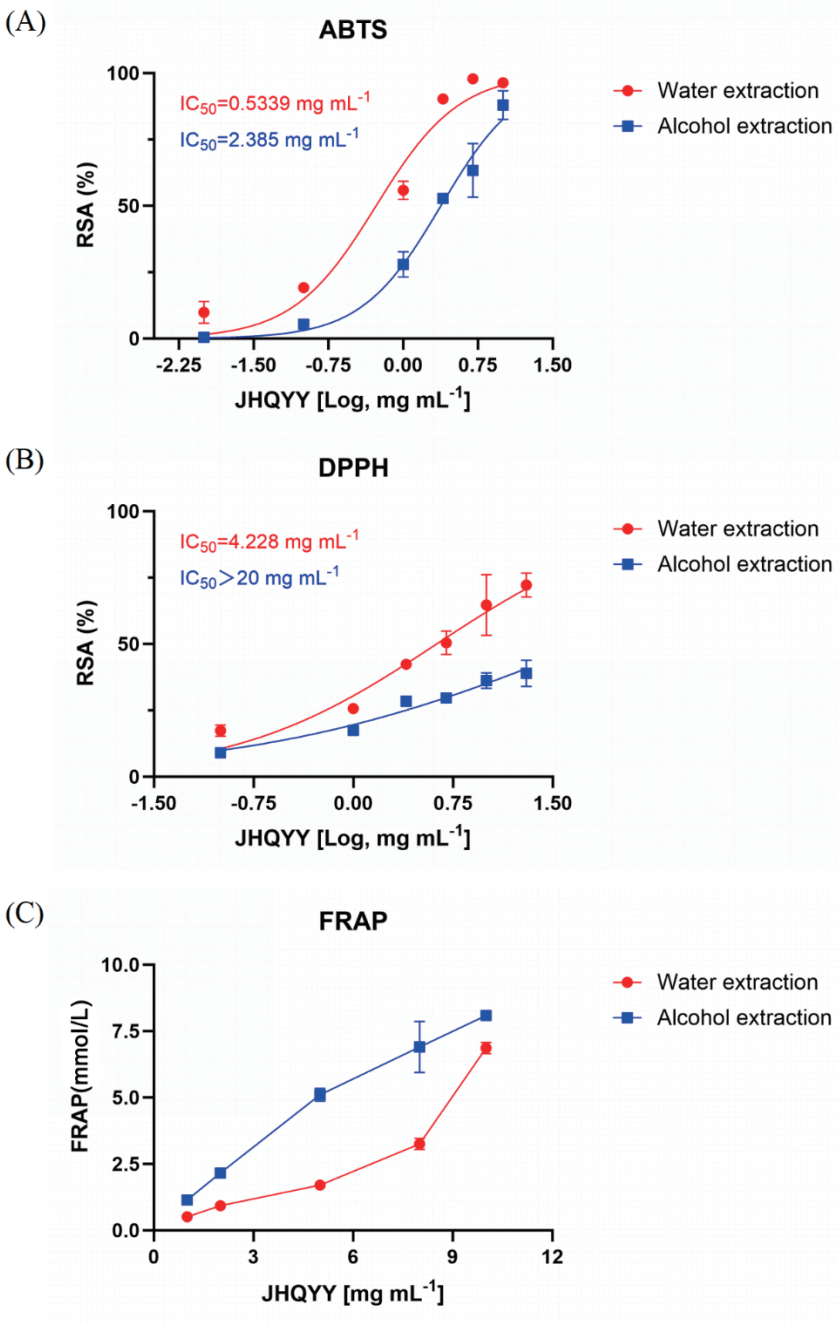

Figure 7 Antioxidant capacity of JHQYY. The red line represents the water extract and the blue line represents the alcohol extract. (A) In ABTS RSA (%), the IC_{50} value of the water extract is 0.533,9 mg/mL, and the IC_{50} value of the alcohol extract is 2.385 mg/mL. (B) In DPPH RSA (%), the IC_{50} value of the water extract is 4.228 mg/mL, and the IC_{50} value of the alcohol extract is greater than 10 mg/mL. (C)The results of FRAP showed that the antioxidant capacity of alcohol extract of JHQYY is higher than that of water extract.

extract (IC_{50} > 20 mg/mL). This suggests that the water extract is more effective in neutralizing $ABTS^+$ and DPPH cation radicals, which are commonly used to assess both hydrophilic and lipophilic antioxidants. The FRAP analysis reveals a distinct difference between the two extracts. The alcohol extract demonstrated a markedly greater ferric-reducing capacity, shown by a more pronounced dose-dependent rise in FRAP values than the water extract. This suggests that polyphenols or flavonoids might be more concentrated in the alcohol extract, possibly accounting for its elevated FRAP levels.

These findings collectively demonstrate distinct antioxidant profiles between the extracts from JHQYY: The aqueous extract excels in scavenging both $ABTS^+$ and DPPH radicals, while the alcoholic extract demonstrates potent electron-donating activity (FRAP), likely attributed to its enriched content of lipid-soluble reducing agents such as polyphenols or flavonoids. The antioxidant capacity measured by FRAP and ABTS is functionally correlated with the cytoprotective effects observed in our cellular model. Oxidative stress triggers lipid peroxidation, compromising cell membrane integrity and causing the leakage of cytoplasmic enzymes like LDH. Furthermore, since ROS serve as key upstream signaling molecules that activate the NF-κB pathway, the extract's radical scavenging capability provides a mechanistic explanation for the observed downstream suppression of pro-inflammatory cytokines (TNF-α, IL-6) in macrophages. These findings suggest that the anti-inflammatory activity of JHQYY may be associated with both NF-κB-related signaling and antioxidant defense.

3.9 JHQYY compound has no toxic effect on RAW264.7 cells

Cytotoxicity assays are widely used to assess the cytotoxic effects of medicinal plants on cells by quantifying cell viability through enzymatic reactions that produce colored substances[46]. In this study, the MTT assay was used to evaluate the effect of the JHQYY compound on the cell viability. RAW264.7 cells were exposed to different concentrations (0, 1, 2, 4, 8 mg/mL) of the JHQYY compound. As shown in Fig. 8, the cell viability in the JHQYY treatment group remained stable with increasing concentrations, with only slight fluctuations in cell survival rates, which consistently remained close to 100%. The result indicated that JHQYY did not significantly affect the cell viability within the tested concentration range. Previous studies have reported that flavonoids (fls) at concentrations ranging from 0 to 100 ng/mL did not significantly alter RAW264.7 macrophage activity[47]. Additionally, a study evaluating a series of high uridine derivatives across 17 target compounds found no cytotoxicity in RAW264.7 cells, with relative cell survival rates exceeding 85% and no cell death observed[48]. The results of this study are consistent with these findings, further confirming the low cytotoxicity of the JHQYY compound and demonstrating its good biocompatibility.

3.10 JHQYY compound inhibited LDH release

LPS induces the activation of immune cells such as macrophages, which not only enhances the inflammatory response but also promotes the excessive release of cytokines, ultimately leading to cellular structural damage and functional loss[49]. Studies have shown that LPS treatment can cause extensive cellular damage and result in the leakage of endogenous enzymes such as LDH, which is a characteristic feature of the inflammatory response[50, 51]. The inhibitory effects of JHQYY on LDH release were evaluated. The results showed that the LDH release increased significantly following LPS stimulation. Compared to the LPS group, the LDH release was reduced after JHQYY treatment (1 mg/mL), with a more significant reduction observed in the 2 mg/mL JHQYY group (Fig. 9), suggesting that JHQYY treatment alleviated LPS-induced LDH release and provided a certain level of cellular protection. Previous studies have found that galectin-1 (gal-1) exerts protective effects by downregulating the release of pro-inflammatory cytokines in LPS-treated macrophages, reducing LDH activity[52]. Additionally, natural compound Obacunone (OB) pre-treatment has been shown to dose-dependently increase cell viability, inhibit LDH release, and promote cell survival[53]. These findings provided experimental evidence supporting the potential of the JHQYY compound as an anti-inflammatory agent.

3.11 JHQYY compound inhibits LPS-induced production of inflammatory cytokines

When macrophages are exposed to external stimuli, they

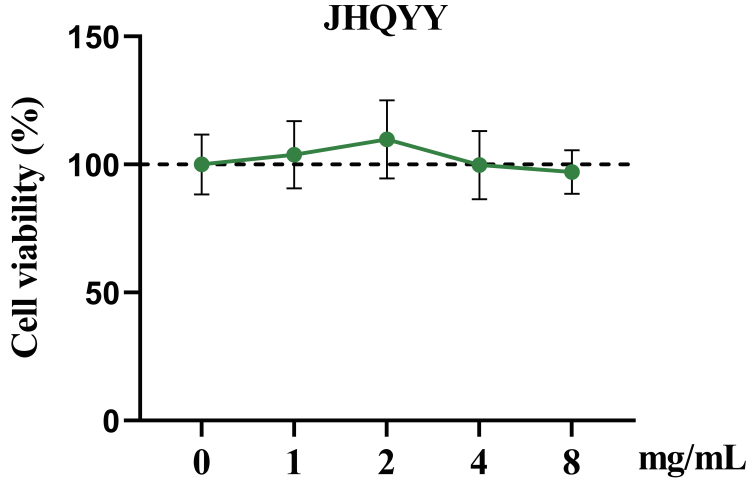

Figure 8 Effect of the JHQYY compound on RAW264.7 macrophage viability. RAW264.7 cells were incubated with different concentrations of the JHQYY compound for 3 h, after which the supernatant was removed. MTT solution and medium were added to each well, and the cells were incubated for an additional 4 h at 37 °C. The cell viability was determined using the MTT cell proliferation and cytotoxicity assay kit.

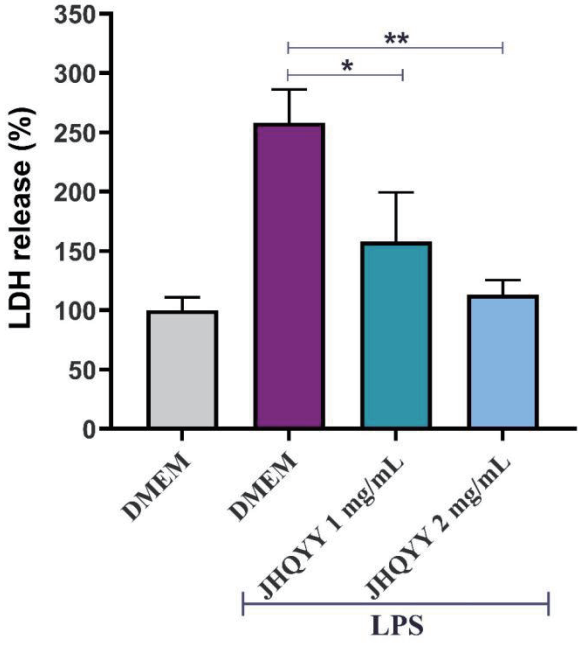

Figure 9 Effect of the JHQYY compound on LPS-induced LDH release (The JHQYY stock solution was prepared in sterile water and diluted with DMEM). RAW264.7 cells were treated with the JHQYY compound (1, 2 mg/mL) for 3 h., followed by stimulation with LPS at a final concentration of 100 ng/mL for 3 h. The culture supernatant was collected, and the LDH levels were determined using the LDH cytotoxicity assay kit. *P < 0.05 and **P < 0.01 indicates statistically significant differences.

phagocytize pathogens and release pro-inflammatory cytokines, which activate other inflammatory cells and recruit them to the site of inflammation[54]. Pro-inflammatory cytokines are primarily secreted by activated macrophages[55]. Through cluster analysis, we found that IL-6, TNF, and IL-1β were identified as key regulators of IBD (Fig. 2). Therefore, these pro-inflammatory cytokines serve as important targets for inhibiting inflammation[56]. After LPS stimulation, the expression levels of IL-1β, IL-6, and TNF-α increased significantly, indicating that LPS effectively induces the expression of inflammatory cytokines. However, after treatment with JHQYY (1 mg/mL and 2 mg/mL), the expression levels of inflammatory cytokines decreased in a dose-dependent manner (Fig. 10). This suggests that the JHQYY compound has an inhibitory effect on LPS-induced inflammatory cytokine expression, with more significant suppression at higher concentrations. Studies showed that compound K, the main metabolite of ginsenoside Rb1 produced by human gut bacteria, can effectively inhibit the release and expression of pro-inflammatory cytokines such as IL-1β and IL-6[57]. Berberine also inhibits LPS-induced macrophage inflammatory responses, and its inhibitory effect on inflammatory cytokines becomes more pronounced with increasing berberine concentration[58]. While *in vivo* models provide macroscopic systemic data, they often introduce complex variables that can obscure direct molecular mechanisms. In strict adherence to the 3Rs principle (Replacement, Reduction, Refinement) of ethical animal research, this study utilized the LPS-induced RAW264.7 macrophage model as a scientifically validated replacement system. This model faithfully mimics the innate immune activation and cytokine storm characteristic of active IBD.

Using the LPS-induced RAW264.7 macrophage model, we demonstrated that JHQYY directly attenuated the inflammatory response at the cellular level, as evidenced by reduced expression of *IL-1β*, *IL-6*, and *TNF-α*. In addition, the newly added *p65*, *CAT*, and *SOD1* gene expression data further support the possibility that this effect is associated with coordinated regulation of NF-κB-related inflammatory signaling and antioxidant defense. However, we acknowledge that the lack of *in vivo* data is a limitation. Future studies will evaluate the systemic efficacy, mucosal healing, and microbiota-modulating effects of JHQYY in DSS-induced colitis animal models.

3.12 JHQYY modulates NF-κB- and antioxidant-related gene expression in LPS-stimulated RAW264.7 macrophages

To further investigate whether the anti-inflammatory activity of JHQYY was associated with NF-κB-related signaling and cellular antioxidant defense, the mRNA expression levels of *p65*, *CAT*, and *SOD1* were determined in LPS-stimulated RAW264.7 macrophages. LPS stimulation markedly increased *p65* mRNA expression compared with the control group, whereas JHQYY treatment significantly reduced *p65* expression, with a stronger inhibitory effect observed at 2 mg/mL (Fig. 11A). In contrast, LPS stimulation suppressed the expression of antioxidant defense-related genes, while JHQYY treatment restored their expression to varying degrees. Specifically, *CAT* mRNA expression was significantly elevated after JHQYY treatment, and the 2 mg/mL group showed a more pronounced increase than the 1 mg/mL group. A similar trend was observed for *SOD1*, whose expression was markedly upregulated by JHQYY in LPS-treated cells

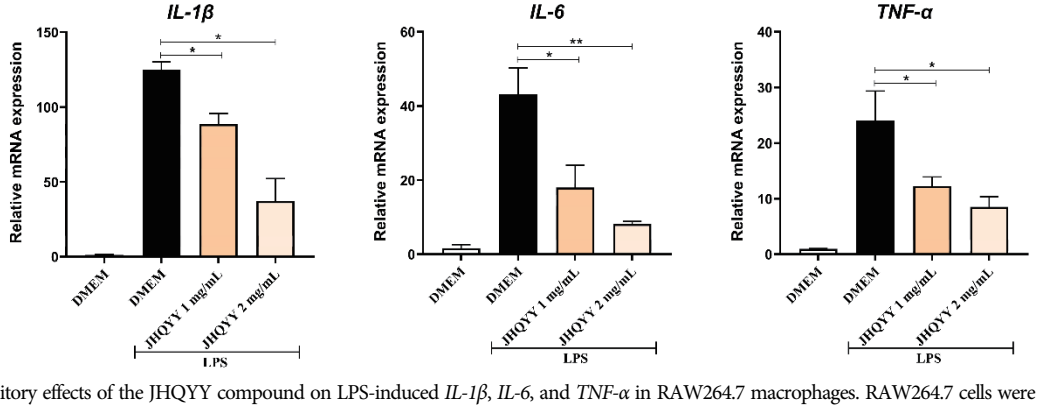

Figure 10 Inhibitory effects of the JHQYY compound on LPS-induced *IL-1β*, *IL-6*, and *TNF-α* in RAW264.7 macrophages. RAW264.7 cells were seeded in 96-well plates, treated with the JHQYY compound for 3 h, and then stimulated with LPS at a final concentration of 100 ng/mL for 4 h. Relative mRNA expression was analyzed by qRT-PCR. *P < 0.05 and **P < 0.01 indicates statistically significant differences.

(Fig. 11B). These results suggest that JHQYY not only attenuates NF-κB-related inflammatory signaling at the transcriptional level, but also enhances the expression of antioxidant enzymes involved in cellular redox homeostasis. The additional gene expression data further support the possibility that JHQYY exerts anti-inflammatory activity through coordinated regulation of inflammatory and antioxidant pathways. p65 is a key transcriptional component of the NF-κB pathway, which drives the expression of multiple pro-inflammatory mediators in IBD and macrophage activation[44]. Meanwhile, CAT and SOD1 are important first-line antioxidant enzymes involved in cellular ROS detoxification, and restoration of their expression is generally associated with improved redox homeostasis and attenuation of inflammation-related oxidative stress[59,60].

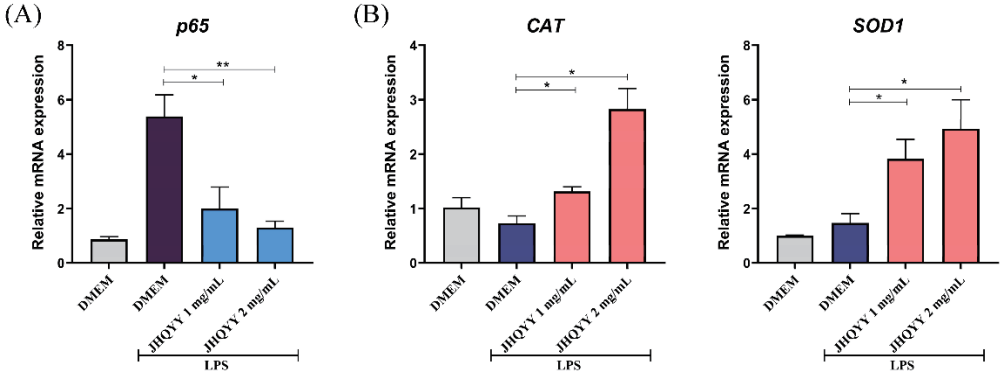

Figure 11 Effects of JHQYY on the mRNA expression of *p65*, *CAT*, and *SOD1* in LPS-stimulated RAW264.7 macrophages. RAW264.7 cells were treated with JHQYY (1 and 2 mg/mL) for 3 h and then stimulated with LPS (100 ng/mL). The relative mRNA expression levels of *p65* (A), *CAT* and *SOD1* (B) were analyzed by qRT-PCR. $^{*}P < 0.05$ and $^{**}P < 0.01$ indicate statistically significant differences.

4 Conclusion

In summary, this study integrated network pharmacology, molecular docking, and cellular experiments to investigate the anti-inflammatory potential of the JHQYY formula. The key active compounds, particularly tea polyphenols, caffeine, vitamin C, and vitamin E, may contribute to the anti-inflammatory activity of JHQYY through multi-target interactions predicted by network pharmacology and molecular docking. The JHQYY compound exhibited low cytotoxicity, notable antioxidant capacity, and effectively reduced LDH release and the expression of pro-inflammatory cytokines in LPS-induced macrophages. In addition, the regulation of p65, CAT, and SOD1 expression further supports the possibility that its anti-inflammatory activity is associated with coordinated regulation of inflammatory and antioxidant pathways. These findings provide preliminary *in vitro* evidence supporting the anti-inflammatory potential of JHQYY. However, the docking-predicted interaction with ALB requires further validation through dedicated binding and pharmacokinetic studies.

Data availability

All data needed to support the conclusions in the paper are presented in the manuscript. Additional data related to this paper may be requested from the corresponding author upon request.

Conflicts of interest

The authors declare that there are no conflicts of interest in this work.

Acknowledgements

None.

Funding

This work was supported by the National Natural Science Foundation of China (32102669), the Natural Science Foundation of Jiangsu Province (BK20210802), and the Postgraduate Research & Practice Innovation Program of Jiangsu Province (SJCX25_2420).

Author contribution statement

Meng-Ru Liu: Writing–original draft, methodology, investigation, visualization, data curation. Yi-Ning Feng: Writing–original draft, methodology, investigation, software. Tao Sun: Methodology, investigation. Bo Wang: Validation, investigation. Wei-Kang Yang: Resources, investigation. Wei Xue: Resources, investigation. Tian-Zhu Guan: Writing–review & editing, validation, supervision, formal analysis, funding acquisition. Dan Xiong: Writing–review & editing, validation, supervision, resources, funding acquisition.

Informed consent

Not applicable.

Ethics statement

Not applicable.

Use of AI statement

None.

References

[1] Liu, S. T., Yu, H., Hou, A. J., et al. A review of the pharmacology, application, ethnopharmacology, phytochemistry, quality control, processing, toxicology, and pharmacokinetics of *Paridis rhizoma*. *World Journal of Traditional Chinese Medicine*, **2022**, 8: 21–49. https://doi.org/10.4103/wjtcm.wjtcm_4_21

[2] Takeuchi, O., Akira, S. Pattern recognition receptors and inflammation. *Cell*, **2010**, 140: 805–820. https://doi.org/10.1016/j.cell.2010.01.022

[3] Fioranelli, M., Roccia, M. G., Flavin, D., et al. Regulation of

inflammatory reaction in health and disease. *International Journal of Molecular Sciences*, **2021**, 22: 5277. https://doi.org/10.3390/ijms22105277

[4] Fullerton, J. N., O'Brien, A. J., Gilroy, D. W. Pathways mediating resolution of inflammation: When enough is too much. *Journal of Pathology*, **2013**, 231: 8–20. https://doi.org/10.1002/path.4232

[5] Min, H. K., Na, H. S., Jhun, J., et al. Identification of gut dysbiosis in axial spondyloarthritis patients and improvement of experimental ankylosing spondyloarthritis by microbiome-derived butyrate with immune-modulating function. *Frontiers in Immunology*, **2023**, 14: 1096565. https://doi.org/10.3389/fimmu.2023.1096565

[6] Koh, T. J., DiPietro, L. A. Inflammation and wound healing: The role of the macrophage. *Expert Reviews in Molecular Medicine*, **2011**, 13: e23. https://doi.org/10.1017/S1462399411001943

[7] Liu, Y., Chen, F., Li, Q., et al. Fish oil alleviates activation of the hypothalamic-pituitary-adrenal axis associated with inhibition of TLR4 and NOD signaling pathways in weaned piglets after a lipopolysaccharide challenge. *The Journal of Nutrition*, **2013**, 143: 1799–1807. https://doi.org/10.3945/jn.113.179960

[8] Bjarnason, I., Scarpignato, C., Holmgren, E., et al. Mechanisms of damage to the gastrointestinal tract from nonsteroidal anti-inflammatory drugs. *Gastroenterology*, **2018**, 154: 500–514. https://doi.org/10.1053/j.gastro.2017.10.049

[9] Grosser, T., Ricciotti, E., FitzGerald, G. A. The cardiovascular pharmacology of nonsteroidal anti-inflammatory drugs. *Trends in Pharmacological Sciences*, **2017**, 38: 733–748. https://doi.org/10.1016/j.tips.2017.05.008

[10] Aravilli, R. K., Vikram, S. L., Kohila, V. Phytochemicals as potential antidotes for targeting NF-κB in rheumatoid arthritis. *3 Biotech*, **2017**, 7: 253. https://doi.org/10.1007/s13205-017-0888-1

[11] Chun, J., Choi, R. J., Khan, S., et al. Alantolactone suppresses inducible nitric oxide synthase and cyclooxygenase-2 expression by down-regulating NF-κB, MAPK and AP-1 *via* the MyD88 signaling pathway in LPS-activated RAW 264.7 cells. *International Immunopharmacology*, **2012**, 14: 375–383. https://doi.org/10.1016/j.intimp.2012.08.011

[12] Feng, X. S., Jia, A. Q. Protective effect of carvacrol on acute lung injury induced by lipopolysaccharide in mice. *Inflammation*, **2014**, 37: 1091–1101. https://doi.org/10.1007/s10753-014-9833-1

[13] Chao, S. C., Hu, D. N., Roberts, J., et al. Inhibition effect of curcumin on UVB-induced secretion of pro-inflammatory cytokines from corneal limbus epithelial cells. *International Journal of Ophthalmology*, **2017**, 10: 827–833. https://doi.org/10.18240/ijo.2017.06.01

[14] Reddy, A. T., Lakshmi, S. P., Maruthi Prasad, E., et al. Epigallocatechin gallate suppresses inflammation in human coronary artery endothelial cells by inhibiting NF-κB. *Life Sciences*, **2020**, 258: 118136. https://doi.org/10.1016/j.lfs.2020.118136

[15] Richard, S. A. Exploring the pivotal immunomodulatory and anti-inflammatory potentials of glycyrrhizic and glycyrrhetinic acids. *Mediators of Inflammation*, **2021**, 2021: 6699560. https://doi.org/10.1155/2021/6699560

[16] Song, X. J., Wang, W., Liu, L., et al. *Poria cocos* attenuates DSS-induced ulcerative colitis *via* NF-κB signaling pathway and regulating gut microbiota. *Molecules*, **2024**, 29: 2154. https://doi.org/10.3390/molecules29092154

[17] Xu, F., Wang, F., Wen, T. Q., et al. Inhibition of NLRP3 inflammasome: A new protective mechanism of cinnamaldehyde in endotoxin poisoning of mice. *Immunopharmacology and Immunotoxicology*, **2017**, 39: 296–304. https://doi.org/10.1080/08923973.2017.1355377

[18] Liu, P. W., Wang, J., Wen, W., et al. Cinnamaldehyde suppresses NLRP3-derived IL-1β *via* activating succinate/HIF-1 in rheumatoid arthritis rats. *International Immunopharmacology*, **2020**, 84: 106570. https://doi.org/10.1016/j.intimp.2020.106570

[19] Tang, S. Q., Wei, K. X., Xu, Y., et al. Network pharmacology combines cellular experiments to investigate the anti-inflammatory phytochemicals of vine of *Pueraria montana* var. *lobata* and their mechanism. *Journal of Ethnopharmacology*, **2025**, 345: 119592. https://doi.org/10.1016/j.jep.2025.119592

[20] Yang, Y., Ding, T. Y., Xiao, G., et al. Anti-inflammatory effects of allocryptopine *via* the target on the CX3CL1-CX3CR1 axis/GNB5/AKT/NF-κB/apoptosis in dextran sulfate-induced mice. *Biomedicines*, **2023**, 11: 464. https://doi.org/10.3390/biomedicines11020464

[21] Qiu, H. J., Liu, M., Wei, Y. Y., et al. The therapeutic target of IBD and the mechanism of dipyridamole in treating IBD explored by GEO gene chips, network pharmacology, and molecular docking. *Endocrine, Metabolic & Immune Disorders-Drug Targets*, **2024**, 25: 230–242. https://doi.org/10.2174/0118715303287122240429092014

[22] Truong, V. L., Bae, Y. J., Rarison, R. H. G., et al. Anti-inflammatory and antioxidant activities of lipophilic fraction from *Liriope platyphylla* seeds using network pharmacology, molecular docking, and *in vitro* experiments. *International Journal of Molecular Sciences*, **2023**, 24: 14958. https://doi.org/10.3390/ijms241914958

[23] Wang, R. Y., Chen, X. M., Gong, S., et al. Interpreting the pharmacological mechanisms of Juanbi recipe on rheumatoid arthritis through network pharmacology and molecular docking. *Annals of Joint*, **2024**, 9: 23. https://doi.org/10.21037/aoj-23-72

[24] Ru, J. L., Li, P., Wang, J. N., et al. TCMSP: A database of systems pharmacology for drug discovery from herbal medicines. *Journal of Cheminformatics*, **2014**, 6: 13. https://doi.org/10.1186/1758-2946-6-13

[25] Tao, Y., Tian, K., Chen, J., et al. Network pharmacology-based prediction of the active compounds, potential targets, and signaling pathways involved in Danshiliuhao Granule for treatment of liver fibrosis. *Evidence-Based Complementary and Alternative Medicine*, **2019**, 2019: 2630357. https://doi.org/10.1155/2019/2630357

[26] Stelzer, G., Rosen, N., Plaschkes, I., et al. The GeneCards suite: From gene data mining to disease genome sequence analyses. *Current Protocols in Bioinformatics*, **2016**, 54: 1.30.1–1.30.33. https://doi.org/10.1002/cpbi.5

[27] Rappaport, N., Twik, M., Plaschkes, I., et al. MalaCards: An amalgamated human disease compendium with diverse clinical and genetic annotation and structured search. *Nucleic Acids Research*, **2017**, 45: D877–D887. https://doi.org/10.1093/nar/gkw1012

[28] Szklarczyk, D., Kirsch, R., Koutrouli, M., et al. The STRING database in 2023: Protein-protein association networks and functional enrichment analyses for any sequenced genome of interest. *Nucleic Acids Research*, **2023**, 51: D638–D646. https://doi.org/10.1093/nar/gkac1000

[29] Morris, G. M., Huey, R., Lindstrom, W., et al. AutoDock4 and AutoDockTools4: Automated docking with selective receptor flexibility. *Journal of Computational Chemistry*, **2009**, 30: 2785–2791. https://doi.org/10.1002/jcc.21256

[30] Liu, X. X., Zhang, L. F., Xu, M. Z., et al. Therapeutic effects and mechanistic insights of YiQiHuangDou decoction on high-fat diet-induced obesity-related glomerulopathy (ORG) in mice. *Journal of Functional Foods*, **2025**, 127: 106728. https://doi.org/10.1016/j.jff.2025.106728

[31] Chemat, F., Rombaut, N., Sicaire, A. G., et al. Ultrasound-assisted extraction of food and natural products: Mechanisms, techniques, combinations, protocols and applications. *A review*. *Ultrasonics Sonochemistry*, **2017**, 34: 540–560. https://doi.org/10.1016/j.ultsonch.2016.06.035

[32] Binsan, W., Benjakul, S., Visessanguan, W., et al. Antioxidative activity of Mungoong, an extract paste, from the cephalothorax of white shrimp (*Litopenaeus vannamei*). *Food Chemistry*, **2008**, 106: 185–193. https://doi.org/10.1016/j.foodchem.2007.05.065

[33] Alzagameem, A., Khaldi-Hansen, B. E., Büchner, D., et al. Lignocellulosic biomass as source for lignin-based environmentally benign antioxidants. *Molecules*, **2018**, 23: 2664. https://doi.org/10.3390/molecules23102664

[34] Yang, L. N., Wang, D. M., Zhou, D., et al. Effect of different isolation methods on structure and properties of lignin from valonea of *Quercus variabilis*. *International Journal of Biological*

Macromolecules, **2016**, 85: 417–424. https://doi.org/10.1016/j.ijbiomac.2016.01.005

[35] Rahman, S. U., Li, Y., Huang, Y. Y., et al. Treatment of inflammatory bowel disease *via* green tea polyphenols: Possible application and protective approaches. *Inflammopharmacology*, **2018**, 26: 319–330. https://doi.org/10.1007/s10787-018-0462-4

[36] Chen, C. H., Wang, H., Hong, T., et al. Effects of tea polysaccharides in combination with polyphenols on dextran sodium sulfate-induced colitis in mice. *Food Chemistry: X*, **2021**, 13: 100190. https://doi.org/10.1016/j.fochx.2021.100190

[37] Jo, H., Lee, D., Go, C., et al. Preventive effect of vitamin C on dextran sulfate sodium (DSS)-induced colitis *via* the regulation of IL-22 and IL-6 production in Gulo(−/−) mice. *International Journal of Molecular Sciences*, **2022**, 23: 10612. https://doi.org/10.3390/ijms231810612

[38] Wu, Q., Luo, Y., Lu, H., et al. The potential role of vitamin E and the mechanism in the prevention and treatment of inflammatory bowel disease. *Foods*, **2024**, 13: 898. https://doi.org/10.3390/foods13060898

[39] Targownik, L. E., Bernstein, C. N. Infectious and malignant complications of TNF inhibitor therapy in IBD. *The American Journal of Gastroenterology*, **2013**, 108: 1835–1842. https://doi.org/10.1038/ajg.2013.294

[40] Souza, R. F., Caetano, M. A. F., Magalhães, H. I. R., et al. Study of tumor necrosis factor receptor in inflammatory bowel disease. *World Journal of Gastroenterology*, **2023**, 29: 2733–2746. https://doi.org/10.3748/wjg.v29.i18.2733

[41] Wu, N. J., Du, Y., Wang, X., et al. Albumin, an interesting and functionally diverse protein, varies from plasma to the short-lived protein in the acutely inflamed brain. *Molecular Medicine Reports*, **2024**, 29: 37. https://doi.org/10.3892/mmr.2023.13147

[42] Schmitt, H., Neurath, M. F., Atreya, R. Role of the IL23/IL17 pathway in Crohn's disease. *Frontiers in Immunology*, **2021**, 12: 622934. https://doi.org/10.3389/fimmu.2021.622934

[43] Kanehisa, M., Goto, S. KEGG: Kyoto encyclopedia of genes and genomes. *Nucleic Acids Research*, **2000**, 28: 27–30. https://doi.org/10.1093/nar/28.1.27

[44] Mukherjee, T., Kumar, N., Chawla, M., et al. The NF-κB signaling system in the immunopathogenesis of inflammatory bowel disease. *Science Signaling*, **2024**, 17: eadh1641. https://doi.org/10.1126/scisignal.adh1641

[45] Liu, G., Yan, W. X., Ding, S. J., et al. Effects of IRW and IQW on oxidative stress and gut microbiota in dextran sodium sulfate-induced colitis. *Cellular Physiology and Biochemistry*, **2018**, 51: 441–451. https://doi.org/10.1159/000495240

[46] Bacanli, M., Anlar, H. G., Başaran, A. A., et al. Assessment of cytotoxicity profiles of different phytochemicals: Comparison of neutral red and MTT assays in different cells in different time periods. *Turkish Journal of Pharmaceutical Sciences*, **2017**, 14: 95–107. https://doi.org/10.4274/tjps.07078

[47] Li, J. L., Chen, J., Huang, P., et al. The anti-inflammatory mechanism of flaxseed linusorbs on lipopolysaccharide-induced RAW 264.7 macrophages by modulating TLR4/NF-κB/MAPK pathway. *Foods*, **2023**, 12: 2398. https://doi.org/10.3390/foods12122398

[48] Pang, L., Liu, C. Y., Gong, G. H., et al. Synthesis, *in vitro* and *in vivo* biological evaluation of novel lappaconitine derivatives as potential anti-inflammatory agents. *Acta Pharmaceutica Sinica B*, **2020**, 10: 628–645. https://doi.org/10.1016/j.apsb.2019.09.002

[49] Feng, J. Q., Ye, S. F., Hai, B., et al. RNF115/BCA2 deficiency alleviated acute liver injury in mice by promoting autophagy and inhibiting inflammatory response. *Cell Death & Disease*, **2023**, 14: 855. https://doi.org/10.1038/s41419-023-06379-7

[50] Zhou, J. B., Wu, K. K., Ma, Y. X., et al. GTS-21 alleviates sepsis-induced atrial fibrillation susceptibility by modulating macrophage polarization and Neuregulin-1 secretion. *International Immunopharmacology*, **2025**, 154: 114561. https://doi.org/10.1016/j.intimp.2025.114561

[51] Leishman, S., Aljadeed, N. M., Qian, L., et al. Fatty acid synthesis promotes inflammasome activation through NLRP3 palmitoylation. *Cell Reports*, **2024**, 43: 114516. https://doi.org/10.1016/j.celrep.2024.114516

[52] Huang, X. T., Liu, W., Zhou, Y., et al. Galectin-1 ameliorates lipopolysaccharide-induced acute lung injury *via* AMPK-Nrf2 pathway in mice. *Free Radical Biology and Medicine*, **2020**, 146: 222–233. https://doi.org/10.1016/j.freeradbiomed.2019.11.011

[53] Li, J., Deng, S. H., Li, J., et al. Obacunone alleviates ferroptosis during lipopolysaccharide-induced acute lung injury by upregulating Nrf2-dependent antioxidant responses. *Cellular & Molecular Biology Letters*, **2022**, 27: 29. https://doi.org/10.1186/s11658-022-00318-8

[54] Arango Duque, G., Descoteaux, A. Macrophage cytokines: Involvement in immunity and infectious diseases. *Frontiers in Immunology*, **2014**, 5: 491. https://doi.org/10.3389/fimmu.2014.00491

[55] Fujiwara, N., Kobayashi, K. Macrophages in inflammation. *Current Drug Targets-Inflammation & Allergy*, **2005**, 4: 281–286. https://doi.org/10.2174/1568010054022024

[56] He, W., Kapate, N., Shields, C. W., et al. Drug delivery to macrophages: A review of targeting drugs and drug carriers to macrophages for inflammatory diseases. *Advanced Drug Delivery Reviews*, **2020**, 165–166: 15–40. https://doi.org/10.1016/j.addr.2019.12.001

[57] Mengeloglu, F., Karakus, K. Thermal degradation, mechanical properties and morphology of wheat straw flour filled recycled thermoplastic composites. *Sensors*, **2008**, 8: 500–519. https://doi.org/10.3390/s8010500

[58] Zhang, S. C., Xu, P. Y., Zhu, Z. W., et al. Acetylation of p65Lys310 by p300 in macrophages mediates anti-inflammatory property of berberine. *Redox Biology*, **2023**, 62: 102704. https://doi.org/10.1016/j.redox.2023.102704

[59] Ighodaro, O. M., Akinloye, O. A. First line defence antioxidants-superoxide dismutase (SOD), catalase (CAT) and glutathione peroxidase (GPX): Their fundamental role in the entire antioxidant defence grid. *Alexandria Journal of Medicine*, **2018**, 54: 287–293. https://doi.org/10.1016/j.ajme.2017.09.001

[60] Hwang, J., Jin, J., Jeon, S., et al. SOD1 suppresses pro-inflammatory immune responses by protecting against oxidative stress in colitis. *Redox Biology*, **2020**, 37: 101760. https://doi.org/10.1016/j.redox.2020.101760